MAGNETOHYDRODYNAMICS Vol. 53 (2017), No. 2, pp. 349–355

2016 YEAR EXPERIMENTS AT RIGA DYNAMO FACILITY

A. Gailitis, G. Lipsbergs

Institute of Physics, University of Latvia, 32 Miera str., LV-2169 Salaspils Latvia
e-Mail: gailitis@sal.lv

The Riga dynamo, a laboratory version of hydromagnetic dynamo, has been rebuilt and is ready for new experiments. The instrumentation for magnetic field and pressure measurements is described. Scaling rules related to the magnetic field amplitude and back reaction in the saturation regime are defined.

Introduction. The Riga Dynamo Facility was built in 1999 for the laboratory reproduction of the common natural phenomenon that the intense motion in a large volume of an electrically conducting fluid produces a magnetic field. This effect is responsible for the magnetic fields of celestial objects. For this laboratory demonstration, $2\,\mathrm{m}^3$ of liquid sodium are moved by a 200 kW powered propeller in an elongated $3 \times 0.8\,\mathrm{m}^2$ annular vessel divided inside into three coaxial channels (Fig. 1). In the central channel, a helical sodium flow runs down, in the middle one it goes straight upwards (blue arrows). The outer sodium volume is immobile. When the volumetric flow rate exceeds $0.6\,\mathrm{m}^3/\mathrm{s}$, a remarkable 0.1 T magnetic field appears seemingly from nothing. The arising screwy field pattern slowly rotates around the vertical axis as long as the sodium moves fast enough.

The last session of experiments produced results that were inconsistent with previous data [1]. The self-generation threshold and the consumed power were considerably increased, and the instability showed a hysteretic behaviour. The growth rates were smaller, and the vertical shapes of the saturated field were also totally different. For that reason, it was decided to renew the whole facility.

Upon disassembling, two main reasons were identified as responsible for the underperformance of the dynamo. Firstly, there were a lot of oxides and other impurities in the propeller zone. Secondly, the 1.5 mm thick shell of the middle volume had a large, almost full-length buckling deformation caused probably by a too large pressure difference applied between the outer and the inner sodium volume. Presumably, this deformation has increased the hydraulic resistance of the channel and changed the structure of the upward back-flow.

Now the facility is renovated, with all three volumes reset to the original condition, and ready for next series of physical experiments. Their main goals are to observe in more detail the field back reaction to the sodium flow and to establish related scaling rules. Measuring techniques for the magnetic field and flow velocity are essential since such results can possibly be used to verify MHD turbulence models of dynamo flows.

1. Modifications made. In order to prevent in the future the encountered mechanical buckling problems, the middle shell of the dynamo module has been reinforced with two axially evenly spaced nonmagnetic rings, welded to the immobile sodium side in order not to disturb the sodium flow. Additionally, gas pressure sensors have replaced the distantly connected manometers for better control of the applied gas pressure to the dynamo module.

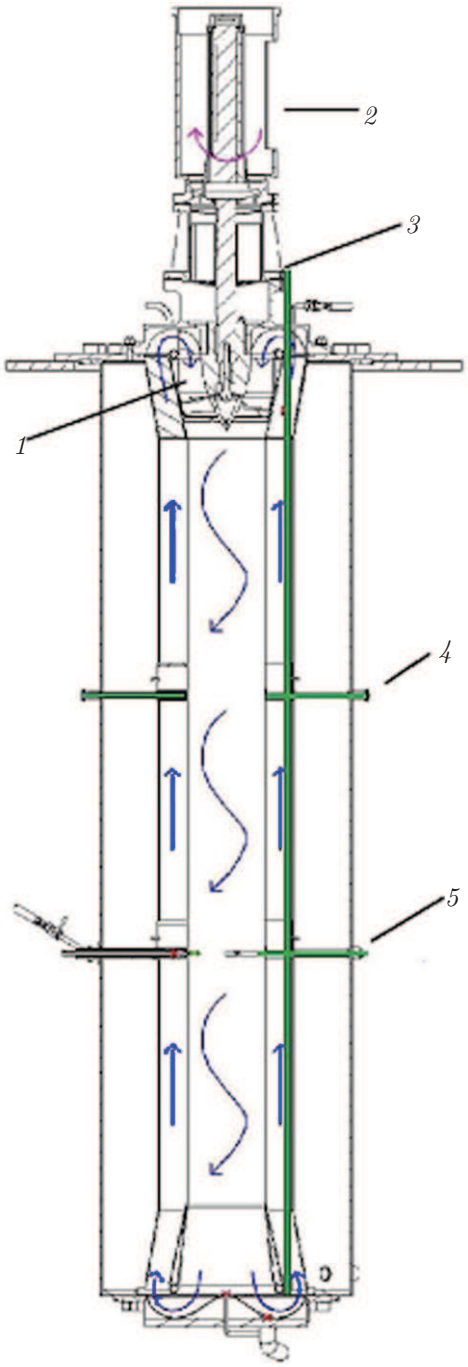

Fig. 1. The dynamo module: *1* – propeller, *2* – magnetic coupler, *3* – vertical measuring port, *4* – upper level ports, *5* – lower level ports.

One reason for the previous oxide build-up could be the uncompleted evacuation of the remaining air as a magnetic coupler which provides the motor power to the propeller was not designed for internal pressure considerably below the atmospheric one. Now the system can be vacuumed prior to filling it with an inert gas due to the specially designed vacuum adapter.

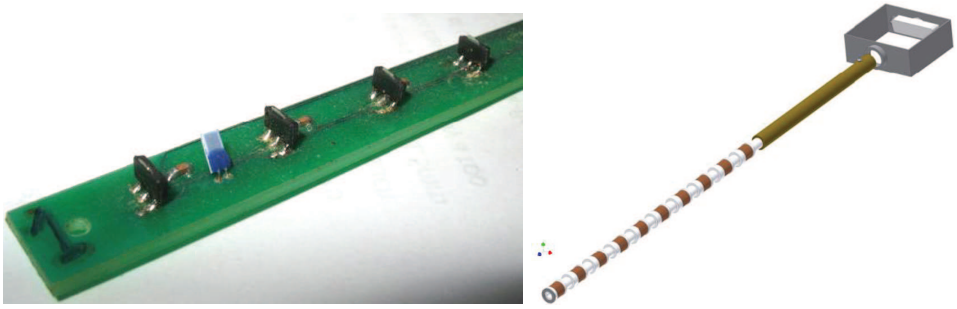

Fig. 2. Magnetic field measuring instruments. A printed plate with radial Hall sensors seen on the visible side, whereas the unseen transverse ones are on the opposite side (left). Radial induction coils (right).

Previous experimental data showed that the sodium temperature increase rate slightly changed when self generation occurred. To be sure that the deviation is real and not just an artefact of the magnetic field induction in a thermocouple wire, we have introduced a Pt100 RTD temperature sensor to provide independent measurement for reference.

1.1. Measurements of magnetic field. To register the magnetic field inside the dynamo, we used 12 probes with a total of 117 sensors. Probes *1*, *2*, *3*, *9*, *10* in Table 1 are made new, probes *4*, *5*, *6*, *7*, *8* remained from previous experiments. Not all of them can operate at once as there are only one vertical port (an outside open channel with the ∅ diameter [mm] in Table 1) and seven radial ports at two different heights in our dynamo module (Fig. 1). At the four blind ports at the upper level which ends at the wall of the central flow, three arrays of Hall sensors were introduced. Each array is comprised of 26 sensors with a temperature-compensated ratiometric[1], linear analog output and a ±100 mT range. Half of them are fixed perpendicular to the arrays plane and measure the field component parallel to the port axis (Fig. 2, left). The others are fixed parallel, on the planes opposite side, and measure the field transverse to the port axis. In this way, each array can be independently set up to measure either the radial (R) and vertical (Z) or the radial (R) and the azimuthal (Φ) components of the dynamo field. Each array is enclosed in a separate tube in order to provide forced air cooling.

Different coreless induction coils were successfully used in previous experiments at the Riga dynamo. They measured time derivatives of the field instead of the field itself which always requires a FFT post processing of recorded data. Another drawback in this setup is the rather small measured signal voltage, a consequence of the low rotation frequency (less than 1.8 Hz) of the magnetic eigenfield in our dynamo. The only way to increase the signal-to-noise ratio is the use of more turns and short individually shielded twisted-pair cables. Two new sets of immobile coreless induction coils with maximized sensitivity were made, one for the radial component, the other for the vertical component (no. 2 and 3 in Table 1, Fig. 2, right).

We have two traversing ports. The horizontal one goes through the dynamo, open at both ends to record the horizontal field profile using probes *6*, *7* or *9*. The vertical port inside the back-flow channel, opened at the top, is used for the measurements of the vertical field profile via the traversing induction probe *8* or Hall probe *10*. This port is located near the outer back-flow wall so that its

[1]For the field in the ±100 mT range, the ratiometric output voltage depends on the supply voltages: $V_{\text{out}} = ((100 - B)V_{\text{sup}}^{-} + (100 + B)V_{\text{sup}}^{+})/200$.

Table 1. Magnetic field probes.

No.	Probe type	Number of sensors in a probe	Measured field component	Number of probes	Used ports (outside open channels, [mm])
1	Hall array	$26 = 13_{\perp} + 13_{\parallel}$	R, Φ or Z	3	4 upper $\varnothing$ 16 ports
2	Radial induction coils	10	R	1	4 upper $\varnothing$ 16 ports
3	Transverse induction coils	10	Φ or Z	1	4 upper $\varnothing$ 16 ports
4	Fluxgate	3	R, Φ, Z	1	4 upper $\varnothing$ 16 ports
5	Tiny induction coils	1	two for R, one for transverse	3	1 narrow $\varnothing$ 5 port combined with a Pitot probe (Fig. 3,left)
6	Induction coils, radially traversing	3	R, Φ, Z	1	1 through going t $\varnothing$ 12 lower port
7	Fluxgate sensors, radially traversing	3		1	1 going through $\varnothing$ 12 lower port
8	Induction coils, vertically traversing	3	R, Φ, Z	1	1 vertical $\varnothing$ 17 port
9	Hall sensors, radially traversing	3	R, Φ, Z	1	1 going through $\varnothing$ 12 lower port
10	Hall sensors, vertically traversing	3	R, Φ, Z	1	1 vertical $\varnothing$ 17 port

influence on the flow is kept to a minimum. The Hall sensors used in probes *9* and *10* are of the same kind as in probe *1*.

In a narrow port via a Pitot velocity probe (Fig. 3, left) a tiny induction coil *5* measures the turbulent structure of the generated magnetic field.

The Fluxgate sensors *4*, *7* are used for detecting weak fields at the level of the Earths field as they are relevant at the very beginning of generation, before and after an experiment, and for the seed field produced by a 3-phase AC excitation coil. The determination of the radial profile of the ambient field and the amplification of the seed field below the self-excitation threshold are particular goals of our research [3].

1.2. Pressure/velocity measurements. We have introduced six points for the flow pressure measurement in the renovated dynamo module. The first pair of points is used in a Pitot type probe for the upward vertical velocity measurement in the back-flow channel. Holes for stagnation and static pressure are coupled with a narrow field measuring port (Fig. 3, left). The pressure sensors themselves are located outside the dynamo.

The second pair of pressure points is meant for the measurement of the azimuthal velocity of the swirl at the bottom of the central channel. One hole is on the axis of the channel, the other is placed on the diameter, where the azimuthal components of the hydrodynamic flow are expected to be the highest. In this way,

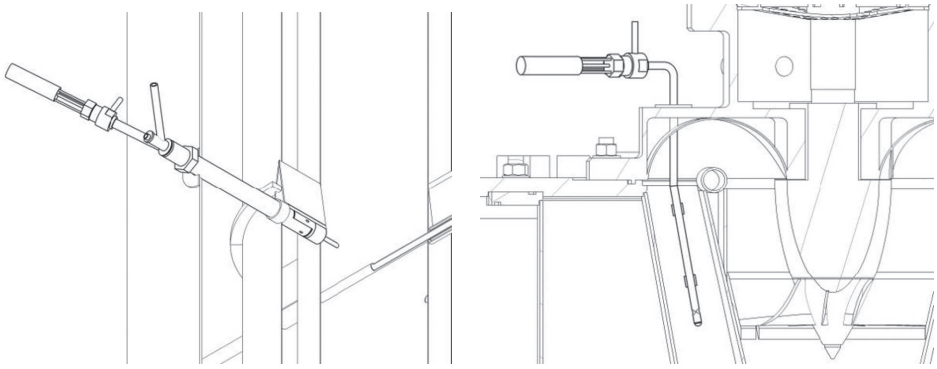

Fig. 3. A Pitot type probe for ascending flow; note two pressure holes and a narrow tip for tiny ∅ 5 induction coil (left), a pressure tube for measuring the induced azimuthal flow, hole marked 'x' (right).

we hope to measure the braking of the flow rotation due to the magnetic field back reaction.

The third pair of pressure points is aimed at measuring the induced azimuthal flow in the upper part of the back-flow channel. Two tubes for pressure measurements are placed on opposite sides of the radially located structural support blade (Fig. 3, right). In the presence of the azimuthal flow there should be a pressure difference.

The used pressure sensors are made by Keller and BD Sensors, with an analogue/digital output. Their temperature range is up to 300°C, suitable for liquid sodium, provided solidification does not take place in contact with the diaphragm.

1.3. Modifications in support system. Instead of three separate sodium tanks used previously one large electrically heated sodium tank of $1.8\,\mathrm{m}^3$ capacity is mounted in the basement. The gas pressure control system is renewed. The sodium filling and draining system, also made anew, is equipped with a sodium filter and two large thermal service ball valves with pneumatic actuator, one for the outer sodium, the other for the inner sodium vessel. This system and also some smaller items are heated by Celduc solid state relays and temperature controllers. Monitoring temperatures are measured and recorded by an NI data acquisition system connected to a dedicated PC. The heating of the module itself is implemented by four vertical U-shaped and one bottom Kanthal rods powered from four 12V DC electric generators.

2. Scaling rules. The determination of scaling rules is one of our main research goals. The field magnitude B in the saturation state is believed to be controlled by the competition between the kinetic energy of the flow and the magnetic field energy. In other words, the relation between the magnetic energy in any fixed location and the kinetic energy should be some dimensionless function F dependent only on the location and on the current propeller rotation rate related to a temperature dependent threshold rate,

$$\frac{n}{n_0(T)}. \tag{1}$$

For a homogeneous dynamo, Eq. (1) is a generation parameter proportional to the magnetic Reynolds number, $\rho(T)$ is the sodium density and L is the principal linear size of the experiment (e.g., the propeller size).

$$\frac{B(\text{location})}{n} = \sqrt{\mu_0\rho(T)}LF(\text{location}, n/n_0(T)). \tag{2}$$

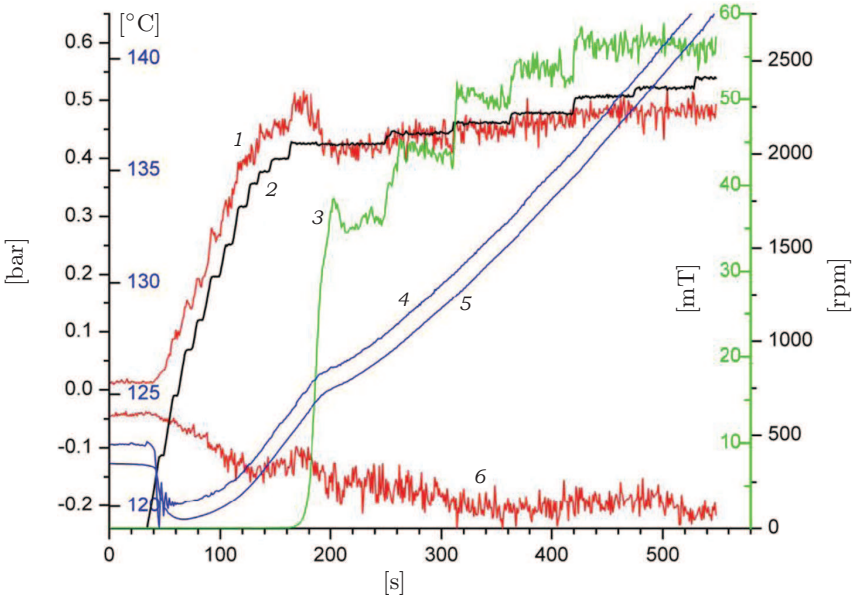

Fig. 4. Magnetic field start-up. *1* – pressure difference on the Pitot probe; *2* – propeller rate; *3* – magnetic field amplitude; *4* – temperature by a thermocouple; *5* – temperature by PT100; *6* – pressure difference at bottom sensors.

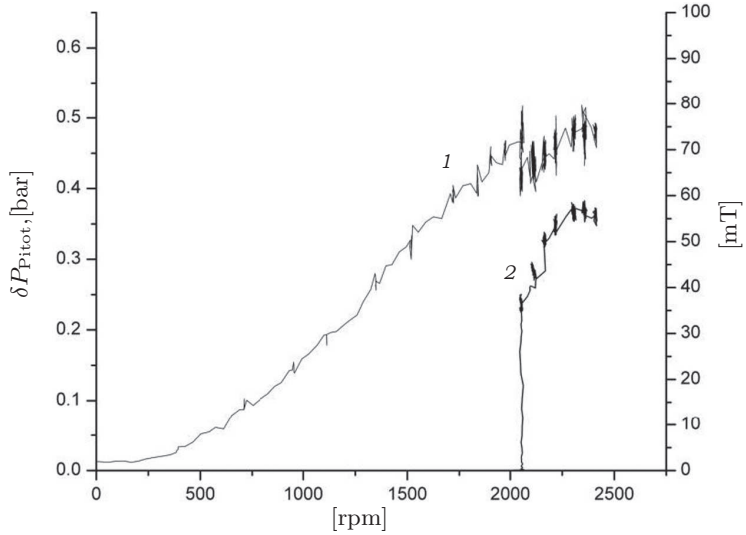

Fig. 5. The pressure difference on the Pitot probe *1* and the amplitude of the magnetic field *2* versus the propeller rate.

Similarly, the relation between the generated pressure difference due to the back reaction of the magnetic field and the kinetic energy should be another function f:

$$\frac{\Delta p(\text{location})}{n^2\rho(T)} = L^2 f(\text{location}, n/n_0(T)). \tag{3}$$

3. Test run. A first run, including the filling procedure and various tests of the control and measurement systems, was successfully accomplished on June 16, 2016. Self-generation of a dynamo eigenfield was achieved at a propeller rate

slightly higher than the expected one. The efficiency of the new measuring system was investigated. At the instant of magnetic field self-excitation both the Pt100 sensor and the Pitot probe confirmed observable changes in temperature increase rate (Fig. 4) and in ascending flow rate (Fig. 5). In contrast, the results of the bottom sensors were less clear.

Acknowledgments. This work was partly supported by the German Helmholtz Association in the framework of the Helmholtz Alliance LIMTECH.

References

[1] A. Gailitis, G. Lipsbergs. Non-standard regimes of the Riga dynamo experiment. In: *Proc. the 8th International PAMIR Conference on Fundamental and Applied MHD* (Borgo, Corsica, France, September 5–9, 2011), pp. 1045–1048.

[2] A. Gailitis, G. Gerbeth, T. Gundrum, O. Lielausis, E. Platacis, F. Stefani. History and results of the Riga dynamo experiments. *Comptes Rendus Physique*, vol. 9 (2008), pp. 721–728.

[3] G. Lipsbergs. Riga dynamo under external excitation. *Magnetohydrodynamics*, vol. 48, (2012), no. 1, pp. 83–90.

Received 06.12.2016